



Enhanced room temperature ammonia gas sensing properties of Al-doped ZnO nanostructured thin films

K. Radhi Devi¹ · G. Selvan² · M. Karunakaran³ · I. Loyola Poul Raj⁴ · A. F. Abd El-Rehim^{5,6} · H. Y. Zahran^{5,6} · Mohd. Shkir⁵ · S. AlFaify⁵

Received: 27 May 2020 / Accepted: 23 October 2020 / Published online: 3 November 2020
© Springer Science+Business Media, LLC, part of Springer Nature 2020

Abstract

In this present research work, we report the preparation of successfully synthesized ZnO films as pristine and doped with Al (Al-ZnO) on glass via facile, eco-friendly, and controllable SILAR method. A systematic evolution of structural, surface morphology, composition, photoluminescence and ammonia gas sensing behaviour of the system was investigated with a variation of Al dopant. XRD examination disclosed polycrystalline nature with the hexagonal system of all films and crystallite size was noticed between 37 and 51 nm. EDX study approves the presence of Al doping in ZnO. Surface morphological tests through SEM presented the formation of nanoparticles and nanorods with a variation of Al content. The photoluminescence study revealed that due to Al doping the PL intensity was quenched which signifies the reduction of defects in the films. It was shown that the estimated values of the energy gap are enlarged to 3.12 from 3.01 on rising the Al content till 3wt.% and finally decreased for 5wt.% Al content. The gas sensing analysis showed that Al doping content was made to drastically increase the gas sensing response. Compared with other dopant levels, the 3wt.% Al-ZnO nanorods unveiled the uppermost retort when tested to 100 ppm ammonia (NH₃) gas concentration at room temperature.

Keywords Controllable SILAR method · Al-ZnO thin films · X-ray diffraction · Optical properties · Gas sensor

✉ G. Selvan
selvan96@redifmail.com

¹ PG and Research Department of Physics, Sethupathy Government Arts College, Ramanathapuram, India

² Department of Physics, Thanthai Hans Roever College, Perambalur, India

³ PG and Research Department of Physics, Alagappa Government Arts College, Karaikudi 630003, India

⁴ Department of Physics, Ananda College, Devakottai 630003, India

⁵ Advanced Functional Materials & Optoelectronics Laboratory (AFMOL), Department of Physics, Faculty of Science, King Khalid University, Abha 61413, Saudi Arabia

⁶ Nanoscience Laboratory for Environmental and Bio-medical Applications (NLEBA), Semiconductor Lab, Department of Physics, Faculty of Education, Ain Shams University, Roxy 11757, Egypt

1 Introduction

Environmental pollution and various hazardous gases released from various chemical factories initiate the scientists to advance chemical sensors able to precisely monitor and alert for industrial and technological related systems in real-time. These developed sensors also can be properly utilized to prevent fire or explosion. Currently, nanostructured metal oxides have drawn significant attention in the field of nanotechnology for making active sensors to solve environmental issues. Semiconducting metal oxide nanostructures (SMONs) are currently focused extensively and play a key role in enhanced gas sensing. These nanostructures are conventional for resistance type gas sensors (Li et al. 2019). When exposed to hazardous gases Nanostructured materials exhibit higher sensitivity and rapid response under relatively low operating temperatures. This fast response might be owed to a large surface/size ratio of nanomaterials particularly in nanoscale, that enhance response kinetics of surface through growing the no. of adsorption centers on the surface of the sensor coating (Dilova et al. 2020). Reducing the grain size to nanoscale may lead to induce new effects such as bandgap widening, room temperature (RT) photoluminescence, etc. due to the quantum confinement (Viter and Iatsunskyi 2019). It is worthy to note that compared to bulk counterparts these nanostructured materials have extraordinary unique and enhanced chemical, physical, and mechanical properties (Nunes et al. 2019). Different morphological structures and shapes also have attained significant interest in employing novel type gas sensor (Aslani 2011). Various patterns like nanoparticles, nanoarrays, nanowires, nanosheets, nanorods, nanotubes, tower-like structures, nanobelts, nanosprings, nanocombs, nanorings and nanofilms, are the latest progress for developing or designing advanced chemical gas sensor (Zhang and Gao 2019; Schmidt-Mende and MacManus-Driscoll 2007). However, for real usages, the key task is focused on discovering low cost, high performance, the sensitive and scalable fabrication process for the manufacture of metal oxide gas sensors.

ZnO is a talented, supreme, and trustworthy material for the above-mentioned purpose. In addition ZnO has prospective application in many fields such as piezoelectric devices (Qin et al. 2016), spintronics (Shaaban et al. 2019), acoustic waveguides (Fu et al. 2010), light emitting diode (Kwon et al. 2018), Photodetector (Liu et al. 2009) photocatalyst (Binjing et al. 2019), solar cells (Linhua et al. 2018), nonlinear characteristics (Sofiani et al. 2007; Abed et al. 2015), etc. Recently ZnO got immense consideration in the gas sensitivity field because of its explicit features, like finest conductivity/low toxicity/cost/chemothermosolidity (Dilova et al. 2020). It also possesses higher mobility, lifetime, and intrinsic impurities. To enhance gas sensitivity V_o , Zn_i , and O_i are possible defects for ZnO material (Schmidt-Mende and MacManus-Driscoll 2007). Nanostructures point of view also it can be easily grown with a variety of nanostructures. ZnO nanostructures have been extensively utilized for proving their excellency in detecting plenty of gases, like $H_2/CO/NO_2/NH_3/H_2S$ /ethanol/acetone etc. (Dilova et al. 2020). The aforementioned gases ammonia is mostly considered as one of the highly toxic gas because of long duration NH_3 inhalation primes to demise (Liu et al. 2019).

Further, based on ZnO-gas sensing devices possess some drawbacks as well like operation at high temperature/limited detection content/selectivity, etc. (Eisele et al. 2001; Stegmeier et al. 2011). Hence, such disadvantages of such sensors limit their use in commercially. To overcome this issue various techniques like doping has been implemented to operate at room temperature in order to surge the efficacy/choosiness and sensitivity of ZnO based sensors. It is worth mentioning that thin film gas sensors that are operated at room temperature (RT)

have many advantages like less power consumption, a long lifetime, and catching fire is not possible (Imad and Kadhim 2016). Generally, group III dopants (transition metals) as Al, Ga, In, Mn, Co, Cr, Ni, Fe, and Cu have been suitably added to improve gas sensing properties. These dopants can boost the oxygen type for sensing and expand gas molecules adsorption (Sankar Ganesh et al. 2017e). Recently, Al dopant is an important candidate, which plays a key role in making ZnO-based gas sensors. This is because Al dopant offers improvement in the gas detection properties of ZnO by changing the energy-band structure, surface morphology, bandgap, transparency, resistivity or conductivity. This alternation is related to small ionic radii of Al^{3+} ion related to Zn^{2+} ion (Aydın and Yakuphanoglu 2019), hence it is called as fast diffusion dopant.

In the past few efforts have been taken by numerous research workers to sense the leakage of various gases by appropriate doping in ZnO. Zhang et al. prepared Al-doped narcissus-like ZnO for NO_2 gas by hydrothermal method. The narcissus-like structure showed a fast response and recovery for the lower operating temperature of 240 °C (Zhang et al. 2019). Ghosh et al. tuned the visible photoluminescence in Al-doped ZnO thin film for detecting the glucose on the basis of quenching in fluorescence. Advanced sensitivity was attained by structure tuning (2018). Sheeba et al. (2017) studied sensing of LPG by a clear Al:ZnO films obtained by the thermo-evaporation process, an appreciable response time of 40 s was achieved for 3 wt.% Al-doped ZnO. Benelmadjat et al. (2013) fabricated highly oriented Al and Al/Sb:ZnO films for H_2 gas on Si wafer by sol-gel method. Rapidly responds to the low H_2 concentrations were noted. Gas detecting action of Al-ZnO film for H_2S recognition was systematically studied by Kolhe et al. (2018) the Al dopant increased the oxygen vacancy related defects, which enhances the gas response at a minimum operating temperature of 200 °C. Madhumita Sinha et al. synthesized quick response/sensing at a low temperature of acetone/ethanol by Al:ZnO, they achieved acetone detection at RT and ethanol detection at a low temperature of 150 °C (Sinha et al. 2020). Aydın et al. (2019) studied the ammonia sensing through Al doping into ZnO for different ppm level in which 5 wt.% Al-doped films operated at room temperature shows the fast response for 660 ppm. Ravichandran et al. (2019) prepared W:ZnO films for sensing of ammonia gas by spray technique, in which 1% tungsten shows a fast response towards 100 ppm ammonia level operated under room temperature.

Up to our knowledge, only a few scientific reports are available for Al-ZnO films which could be operated at RT to detect NH_3 gas. Moreover, fast response and recovery time is necessary to detect a low-level concentration of such harmful gas. So, to achieve these two objectives, we synthesized Al-ZnO films for the NH_3 sensor by the SILAR method. Compared with several other techniques SILAR technique is preferred most because this promising route has the following advantages such as simplicity, non-hazardous, inexpensive, less time consuming, does not require sophisticated instruments and high-quality substrates, easy route for the introduction of different dopants, suitable for large areas deposition and also to build functional structures (Deshmukh et al. 2018; Raut et al. 2017; Omran et al. 2019). So, current work is focuses to fabricate Al-ZnO films via SILAR process and investigate their characteristics towards ammonia gas sensing.

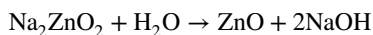
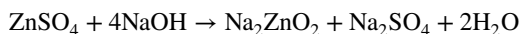
2 Investigational procedures

2.1 Preparation on Al-ZnO thin films

Here SILAR technique was adopted for the deposition of Al-ZnO thin films on glass slides. Zinc sulfate [ZnSO₄], NaOH, and Hexahydrate aluminium chloride (AlCl₃ 0.6H₂O) were collected from locally available commercial markets in India and they were used without further purified. In order to remove the visible dirt, all the glass slides were initially cleaned with soapy water. Then they were successively washed with chromic acid, well rinsed with deionized water and then dried.

To deposit the films the cleaned substrates were vertically dipped into the sodium zincate solution, which can be prepared by mixing 0.1 M ZnSO₄ and 0.2 M NaOH. Before dipping the temperature of this solution was maintained at 90 °C. The pH of sodium zincate solution bath was maintained at 9. After immersing the substrate for 10 s in a sodium zincate bath, it was immersed in hot water (90 °C) for 10 s. This course was repetitive for 80 times to get pristine ZnO films. Aluminium doping was done by adding hexahydrate aluminium chloride at different proportions of Al, such as 0, 1, 3, and 5 wt.%. After the completion of the dipping cycles, the substrates drying was done in the air and then annealed at 400 °C for about 2 h.

The equations for the formation of ZnO thin films are as follows:



2.2 Characterization

The prepared high-quality ZnO thin films were analyzed and recorded to recognize their phase, morphology, composition, and most importantly ammonia gas sensing behaviors affected by Al content. The structure information of undoped and Al-ZnO films was obtained by XRD (Bruker D8 Advance Eco XRD). A scanning electron microscope (EVO18 CARL ZEISS) was employed to investigate the evolution of the morphology of samples. The room temperature Photoluminescence (PL) data were collected using a Varian Carry Eclipse PL Spectrometer. The optical properties were accessed through Ocean Optics HR 2000 optical fiber-based spectrophotometer. Stylus profile meter (Mitutoyo SJ-301) was employed to determine the thickness of prepared films and are noted to ~ 920, 980, 1020, and 880 nm for 0, 1, 3, and 5 wt.% of Al dopings, respectively.

3 Result and conversation

3.1 XRD studies

Figure 1 depicted detailed XRD profiles of pristine and Al-ZnO films. From Fig. 1 we noted that the nature of all films is polycrystalline and exhibited multiple peaks with hexagonal structure. Moreover, it is strongly oriented along the (002) direction.

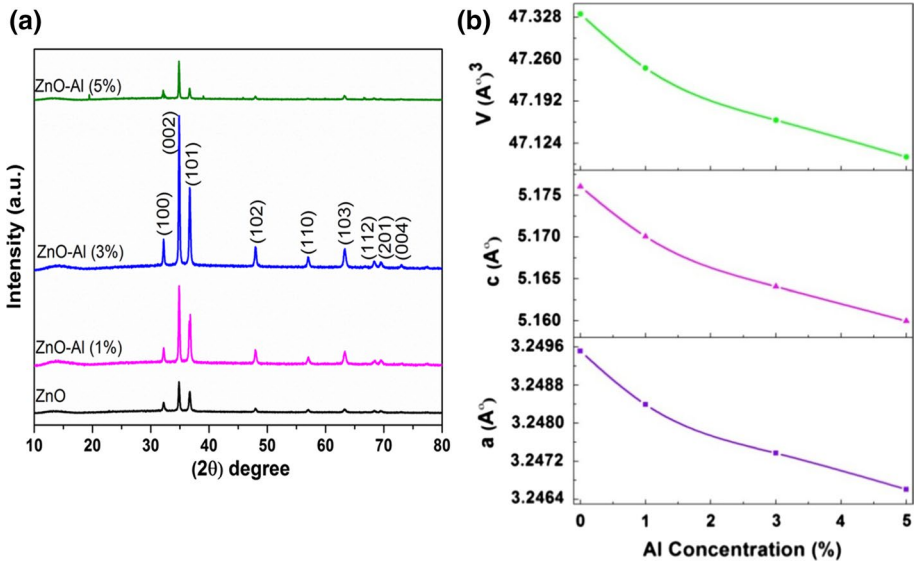


Fig. 1 **a** X-ray diffraction patterns of Al-ZnO thin films with different Al doping concentrations. **b** Lattice parameters of Al-ZnO thin films with different Al doping concentrations

This strongest peak is usually observed in ZnO thin films suggesting that free energy of the surface of (002) plane is the lowermost in ZnO films (Fidal and Chandra 2018; Taabouche et al. 2016). The other diffraction peaks correspond to (100), (101), (102), (112), (103) (112) and (201) orientations also appeared. All the diffraction peaks of ZnO which matched with the JCPDS card no. 005–0664 (Linhua et al. 2014). All appeared diffraction peaks are sharp and well distinct which suggests the formation of high-quality crystalline phase of ZnO. No additional secondary phases related to Al or Al_2O_3 species were occurred not even for the highest proportion. Hence, we assumed that Al^{3+} substituted into the Zn^{2+} sites/incorporated interstitially in host ZnO lattice with unchanged hexagonal structure crystal structure (Humayan Kabir et al. 2018). This may indicate that the precursors have been fully converted into ZnO phase (Sinha and Mahapatra 2020). The intensity of (002) and (101) planes increases with increasing the Al concentration up to 3% doping concentration confirms the incorporation of Al atoms into ZnO lattice and its crystallite size was increased. Furthermore, for 5wt.% Al concentration the peak intensity is considerably decreased due to Al atoms placed in interstitial position or surface of the grains causes structural disorder in the crystal structure. A decrease in the crystallite size was an indication of deterioration of the crystallinity of the films. A similar type of observation was reported by Kamal Rudra et al. for Mn doping of nanostructure ZnO (Kamal Rudra and Prajapati 2020). Goktas et al. also reported the same type of observation for various transition metal dopants like Mn, Co, Fe into ZnO film (Goktasa et al. 2016).

The structural constraints like size of crystallites (D), micro strain (ϵ), number of dislocations (δ) and quantity of crystallites (N) were evaluated by (Deva Arun Kumar et al. 2018)

$$D = \frac{0.9\lambda}{\beta \cos \theta} \quad (1)$$

$$\varepsilon = \frac{\beta \cot \theta}{4} \quad (2)$$

$$\delta = \frac{1}{D^2} \quad (3)$$

$$N = \frac{t}{D^3} \quad (4)$$

Here all codes are well-recognised.

It has been noticed that the crystallite size became bigger when the concentration of Al reached 3wt.% then leads to a decrease for 5wt.% Al level. The undoped ZnO possesses the smallest crystalline size. The FWHM of XRD peaks decreases firstly then rises on rising of Al impurity content, which supports the variation of crystallite size. The calculated crystallite size is comparable with previously reported values by Zaiour et al. (2019). The calculated microstrain and dislocation density values are low for 3wt.% Al content which indicates the formation of fewer defects. The N values initially declined and finally enlarged with Al impurity. Table 1 shows the calculated structural parameter values.

The cell volume 'V' and lattice constants 'a' and 'c' are evaluated for (002) peak by Vijayprasath et al. (2014).

$$v = a^2c(\sin 60^\circ) \quad (5)$$

$$\frac{1}{d^2} = \frac{4}{3} \left\{ \frac{h^2 + hk + k^2}{a^2} \right\} + \left\{ \frac{l^2}{c^2} \right\} \quad (6)$$

here (hkl) and d have their usual meanings. The calculated lattice constants 'a', 'c' and 'V' for Al- ZnO films were depicted in Fig. 2b revealed that the cell volume has been decreased with Al doping and the highest value was noticed for undoped ZnO. It is noticed that a rise in Al content roots the decrement in both *a* and *c* parameters. This is due to the small ionic radius of Al³⁺ (0.68 Å) to the ionic radius of Zn²⁺ (0.74 Å). The change in the lattice parameter suggesting the formation of uniform strain (Hong and Choi 2018). The estimated lattice parameter values comparable with earlier data reported by Osali et. al. (*a*=3.25 Å and *c*=5.207 Å) (Osali and Karami 2018).

Table 1 Film thickness, structural parameters and bandgap of SILAR deposited Al-ZnO thin films

Al concentration (wt.%)	Film thickness (nm)	Crystallite size (nm)	Dislocation density ($\times 10^{15}$) lines.m ⁻²	Strain ($\times 10^{-3}$)	Number of crystallites ($\times 10^{16}$ m ⁻²)	Bandgap (eV)
0	920	37	0.750	3.18	1.89	3.01
1	980	41	0.583	2.80	1.38	3.04
3	1020	51	0.378	2.25	0.75	3.12
5	880	45	0.504	2.60	0.99	3.09

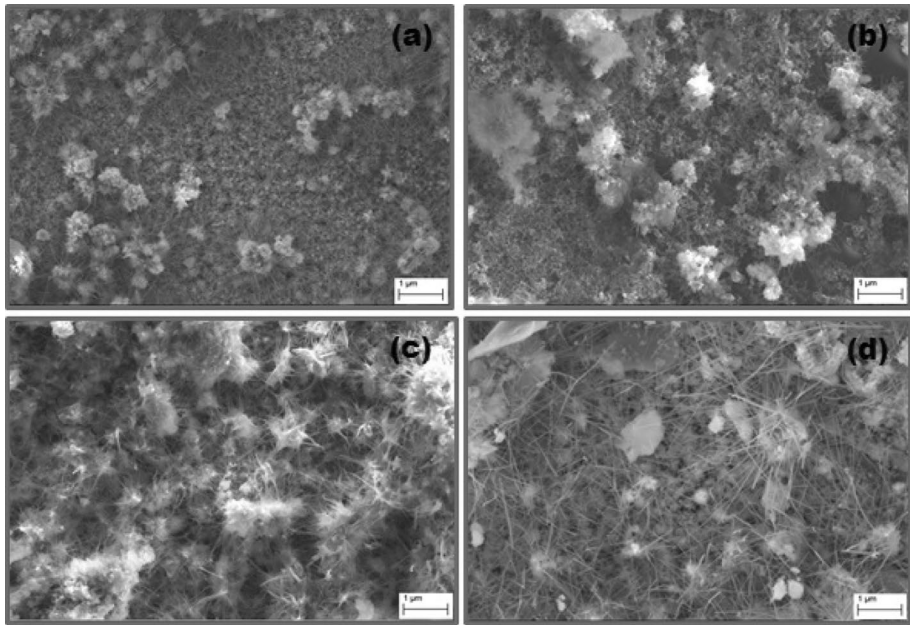


Fig. 2 SEM images of **a** pure, **b** 1, **c** 3 and **d** 5 wt.% Al-ZnO thin films

3.2 Morphological studies

Figure 2a–d provided the surface morphological images of as-deposited Al-ZnO films. Some notable changes between the samples were observed as the doping percentage of Al content increases. It can be observed that the surface of the un-doped film has been covered with nano. From Fig. 2b, it is observed that film contains small size nanowire like morphology. However, with 3wt% Al doping, the film morphology is completely nanowire shape [see Fig. 2c] is very clear, which may be due to higher concentration doping of Al. The 5% doped film exhibits an entire wire-like nanostructure and its size is higher than previous samples. It is worthy to note the increment in the length of the nanowire has been observed. Moreover, a small difference was observed in all the upper parts of the fabricated films. The highly packed particles are observed on the surface of pure ZnO film along with few particles on top leads to agglomerate. These suggest that Al impurity is deposited preferably on the upper parts of ZnO which leads to the formation of a nano wire-like structure. Yuanyuan Lv et al. (2018) fabricated ZnO Nanowire by influencing Al dopant into the host lattice of ZnO. Antaryami Mohanta et al. (2019) also prepared ZnO nanowires through Al addition. F:ZnO NWs achieved by plasma action was reported by Wang et al. (2018). Kim et al. (2019) formed Pd on ZnO NWs for improved sensitivity/selectivity towards H₂ gas. Room temperature gas nanosensors based Au-modified ZnO nanowires synthesized by Lupan et al. (2019). Mohd Arif et al. (2019) applied Sol–gel spin coating to fabricate the pure and different concentrations of aluminum-doped ZnO nanostructure. Sankar Ganesh et al. (2017e) tune the response of NH₃ sensing through Cu-in ZnO. Hence it is worth to our nano wire-like morphology results also resembles these results.

The elemental analysis of Al-doped thin films was achieved by EDX is projected in Fig. 3. The EDX spectrum obtained for the SILAR prepared ZnO thin film deposited with

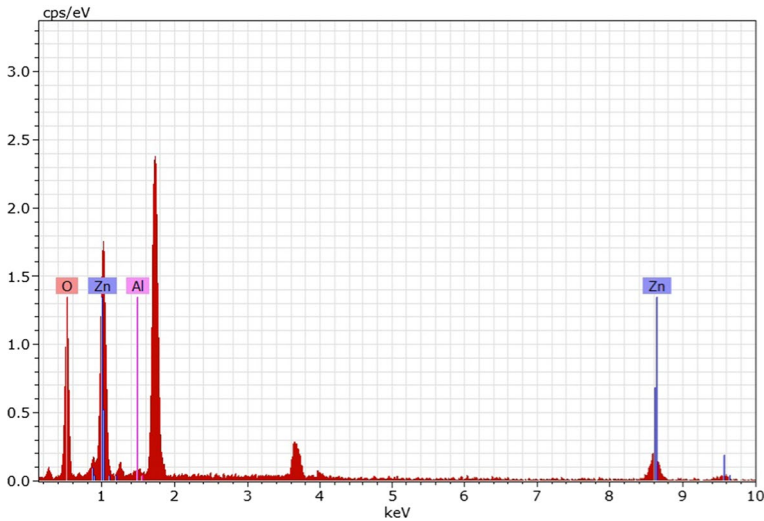


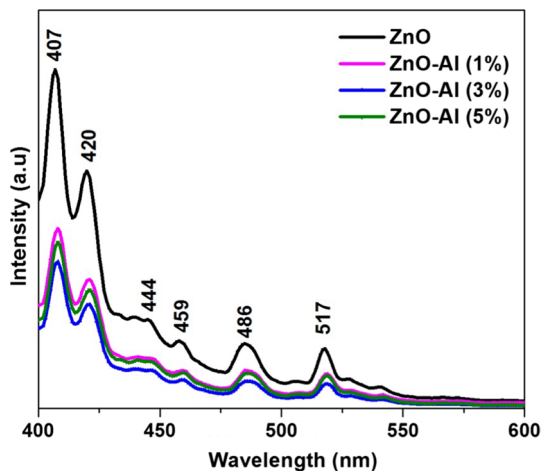
Fig. 3 EDX spectrum of Al-ZnO(3wt.%) thin film

3wt.% Al which confirmed that Zn, O, and Al elements have emerged within the structure. The appearance of additional peaks may be owing to the glass substrate.

3.3 Photoluminescence studies

PL spectroscopy is an inevitable tool to analyze Photoluminescence behavior because it furnishes more information about sensing behaviors, point defects, and band edge emissions. Figure 4 displays RT PL spectra of Al doped ZnO films, which signify that luminescence character dependency on Al content. On increasing Al content emission intensity reduced to 3 wt.%, however, increased for 5 wt.%. Two intense PLE bands exist in all films

Fig. 4 Photoluminescence spectra of Al-ZnO thin films with different Al doping concentrations



from which one is for NBE occurs owing to recombining the excitons among CB and VB. Figure 4 contains 4 sharp peaks at 407, 420, 486, and 517 nm and two small peaks at 444, and 459 nm total of six defects were presented. Generally, six kinds of intrinsic imperfections are likely names as V_O , Zn_i , O_i , Zn_v , and Zn/O antisite (Nkosi et al. 2020). Moreover, it is worthy to note that the presence of defects and vacancies are beneficial for gas sensing applications (Patil et al. 2019). The PLE band at ~406 nm is for NBE, the other PLE bands at 458 and 484 nm are ascribed to Zn_i and at 540 nm is for V_O . The low-intensity blue PLE at 445 nm is for Zn_i , an intense PLE band at 518 nm (green) is for V_O (Anita et al. 2016; Renitta and Vijayalakshmi 2017). Normally higher the ZnO crystal quality possesses stronger UV emission (Ahmed et al. 2019). It can be known from XRD patterns that 3 wt.% Al doped ZnO shows the strongest diffraction peak; e.g. some ZnO with better crystallinity like NRs, NWs possess an exceptional UV emission act (Linhua et al. 2019).

3.4 Optical studies

A detailed study on optical transmittance can be used to analyze the effect (optical energy bandgap, optical transitions) of Aluminium dopant on the optical nature of ZnO film. Figure 5a demonstrates the optical transparency for Al-ZnO films prepared with various Al concentrations. All samples exhibit average transmittance values between 30 and 82%, depending on the dopant concentrations in the visible wavelength region. While increasing Al in ZnO the transparency is enhanced significantly in VIS-region. The 3 wt.% Al-ZnO film exhibits the highest transmission, whereas the lowest one around 30% is shown by the undoped film. This maximum optical transmittance spectrum specified that the Al-ZnO films can have good structural homogeneity (Hou and Jayatissa 2017). Compared to 5% Al-ZnO films, the film doped with 3 wt.% shows slightly increasing transmittance values shows a maximum optical transmission which indicates the degradation in the crystal quality for higher doping. It is matched with XRD results. These transmittance findings are perfectly matched with the workers Musaab Khudhr et al. (xxxx), Zhai et al. (2016), and Mkawi et al. (2015). Further, a drop in T is observed in all the prepared films at around 400 nm. This drop may be due to the fundamental absorption by excitonic transitions.

The E_g values were estimated via Tauc's rule (Firdous et al. 2013)

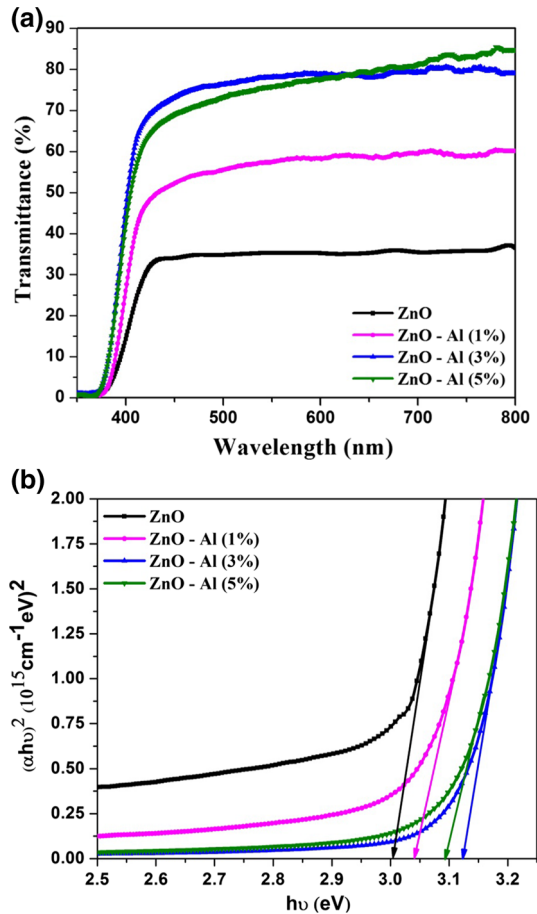
$$\alpha hv = B(hv - E_g)^n \quad (7)$$

Here, α is the coefficient of absorption, E_g is the direct energy gap, and B is a constant. The inset in Fig. 5b displayed the attained E_g of all Al-ZnO films. As can be seen from Fig. 5b the E_g value of undoped ZnO film was found to be equal to 3.01 eV. When the Al concentration is increased up to 3wt.% the E_g value is enlarged from 3.01 to 3.12 eV then finally decreased for a higher doping level. This result is in accordance with the report of Rajendra Prasad et al. (Rajendra Prasad and Haris 2018).

3.5 Gas sensing studies

An indigenously designed set-up (Keithley) was employed to investigate the sensing act of undoped and Al-ZnO films. A High-quality Ag paste was used to make contacts on the surface. The sensing element kept in the sensor testing chamber. Baseline resistance was noted at RT for the Al-ZnO sensor by keeping an open chamber to allow atmosphere air. Then ammonia is injected by syringe to the tube which is connected by

Fig. 5 **a** Transmittance and **b** Bandgap spectra of Al-ZnO thin films with different Al doping concentrations



a heater. Ammonia vapour is produced by applying the required heat to the tube that relates to film and so lessening resistance. All sensor-related tests are done at RT by keeping the sensing area constant. For sensing of gas, the applied voltage was fixed at 5 V. Sensitivity is defined by Sivalingam et al. (2012): $S = R_a/R_g$, where R_a and R_g are strengths of air and gas (Table 2).

Figure 6 reveals the response/recovery of Al-ZnO (0, 1, 3, and 5wt. %) films for 100 ppm of NH_3 gas. The observed timings of responses are 52, 47, 34, and 39 s, and recoveries are 11, 10, 6 and 9 s for Al-ZnO (0, 1, 3, and 5wt. %) samples, respectively. The observed response time initially increased on rising Al doping content in ZnO and maximum response time was observed for 3 wt% Al-doped film due to high crystalline and nanowire structure. The sensitivity of the samples is 547, 6470, 10,700, and 12,300 for Al (0, 1, 3, and 5wt. %) doped ZnO film. The excellent sensitivity observed for Al 3wt.% film rather than other doped films due to its high crystalline quality and nanowire structure is suitable for diffusion and interaction of more ammonia vapours. Figure 7 elaborates sensing features of 3wt.% Al-ZnO film for diverse contents of NH_3 at RT operating condition. Sensitivity increases as increasing ammonia vapour ppm from 100 to 200. It is clear from the observations that the amount of vapour interact on the surface of Al-ZnO films is a

Table 2 NH₃ sensing towards various metal doped ZnO by different methods

S.No	Material	Structure	Operating temperature	Concentration	Sensing temperature	Response time	Recovery time	Response	References
1	Pure ZnO	Thin film	350 °C	200 ppm	–	–	–	–	Nanto et al. (1986)
2	Pure ZnO	Thin film	400 °C	100 ppm	RT	120 s	10 s	–	Ravichandran et al. (2016)
3	Pd doped ZnO	Thin film	200 °C	30 ppm	–	198 s	334 s	–	Mhlongo et al. (2015)
4	In doped ZnO	Thin film	300 °C	10 ppm	–	40 s	100 s	–	Sberveglieri et al. (1995)
5	Yt doped ZnO	Thin film	R.T	100 ppm	–	110 s	101 s	–	Vinoth and Gopalakrishnan (in press)
6	Ba doped ZnO	Nano thin film	400 °C	600 ppm	250 °C	130 s	40 s	17.9	Gopala Krishnan and Elango (2018)
7	Mn doped ZnO	nanoparticles	150 °C	20 ppm	–	4 s	10 s	–	Sankar Ganesh et al. (2017a)
8	Ru doped ZnO	Thin film	250 °C	1000 ppm	–	18 s	960 s	386	Wagh et al. (2006)
9	Al doped ZnO	Thin film	R.T	100 ppm	RT	39 s	9 s	–	Present work

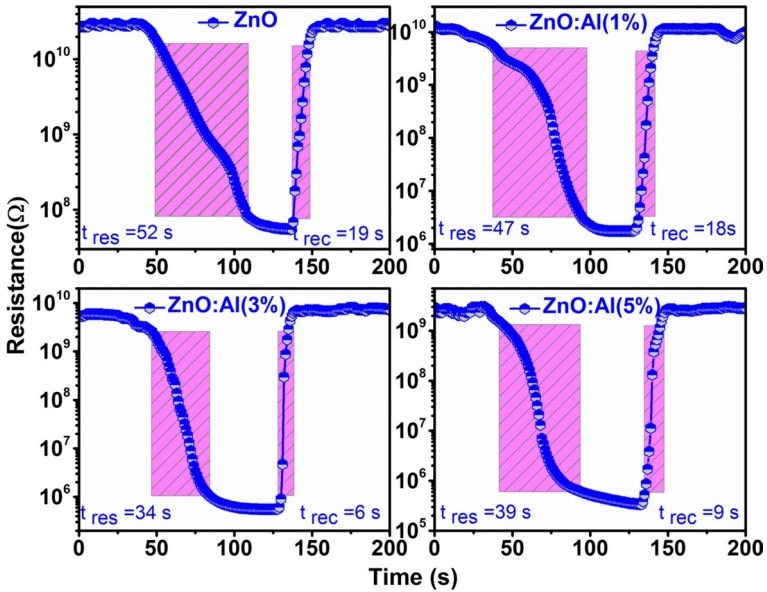
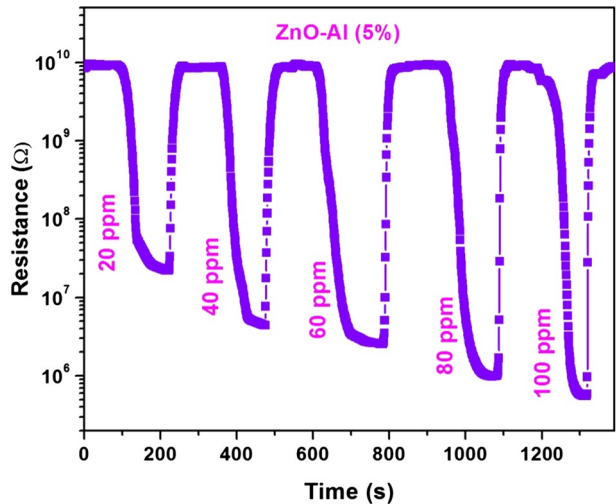


Fig. 6 Response time (t_{res}) and recovery time (t_{rec}) of Al-ZnO thin films deposited on glass substrate with exposure and removal of NH_3 gas of 100 ppm concentration condition

Fig. 7 Gas response of Al-ZnO (5%) thin film deposited on glass substrate with exposure and removal of NH_3 gas with different ppm



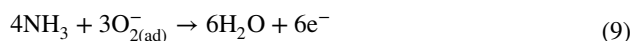
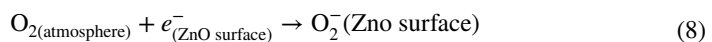
vital constraint governing the response. It is also confirmed from the figure that Al-ZnO display an enhancement in the sensitivity and high selectivity for ammonia.

The observed value of response and recovery time of present work is compared with other works. Sankar Ganesh et al. (2017d) synthesized enriched of NH_3 gas sensor as Ag/ZnO by hydrothermal method. They showed that the addition of Ag exhibited quick response/recovery timings of 13/20 s for operating temperature 150 °C. On the other hand,

Fairose et al. (2019) lessened the response/recovery timing to 8/37 s through a nanostructured ZnO sensor by the SILAR method but the operating temperature of the sample was 200 °C which is higher than our work. Ravichandran et al. (2019) studied room temperature ammonia vapour sensing ability for tungsten doped ZnO. The loaded tungsten showed a response and recovery time of 293 s and 13 s for the 100 ppm level. This achievement was due to a greater number of V_o and Z_i these are the key reasons for the enrichment of sensing capability. But Kulandaisamy et al. (2016) reduced the response and recovery time up to 34 s and 28 s by introducing Mg into ZnO host lattice. This room-temperature sensing nature might be because of lesser grain size. Ganesh Kumar Mani et al. (2014) attained much better performance than those already discussed so far with a quicker response/recovery of 30/14 s for room temperature ammonia sensor for 50 ppm. Smaller grain size reflected faster response/recovery time. Thus, compared to the above-mentioned reports the Al-ZnO film is showing a best response/recovery time of 34/9 s for 100 ppm. This fast response is might be because of the generation of nanowire like morphology formed by Al content. Mariappan et al. (2014) reported Na-ZnO NRs films by NSP and their HN_3 sensing activity. The uniformly distributed nanorods show the sensing response of 1.7 for 500 ppm operated at 400 °C. Sankar Ganesh et al. (2017a) increased the sensitivity of 15.1 for the operating temperature of 400 °C when exposed to 100 ppm. It was due to enhanced catalytic activity. On the other hand Pt nanoparticles (NPs) are deposited on a sputtered aluminum-doped zinc oxide exhibited a sensing response of 2183 once exposed to 1000 ppm but the working temperature was 300 °C by Chen et al. (2018). Mani et al. (2015) presents a very selective co-doped ZnO RT NH_3 sensor. Its sensing response was 225. Sankar Ganesh et al. (2017b) investigated the influence of Al doping on RT ammonia sensing by ZnO nanorods. It displayed a fast sensing response of 350 owed to the existence of frequent V_o , which indorses oxygen adsorption. In current, we accomplished a high response of 12,300 towards RT NH_3 sensing due to the nanostructure of nanowire-like structure. Furthermore, we have listed some work that was reported and published already.

3.5.1 Sensing mechanism

Figure 8 presents the mechanism for NH_3 sensing towards pure and 3wt. % Al-ZnO films. The sensing of NH_3 behavior is primarily built on chemical reactions amongst test gas and targeted specimen. This process might be discussed in 2 main steps. Initially, when the undoped ZnO thin film was bare to ambient air, oxygen molecules were captured by electrons apprehending from CB of ZnO. As a result, the width of the potential barrier changed which leads to an increase of resistance. It is expressed through Eq. (8), once plummeting gas like NH_3 is exposed to ZnO films surface, NH_3 vapours interact its surface adsorbed oxygen, and electrons gets freed to surface, thus reduces the width of the potential barrier. Consequently, the resistance decreases and gas sensing response increases. This express able by Eq. (9) (Rana and Rajasree 2016; Kanaparthi and Singh 2020).



Similarly, 3wt.%Al-doped ZnO film contains more nanowires causes, more oxygen species can interact than undoped ZnO film thus the depletion layer width is reduced.

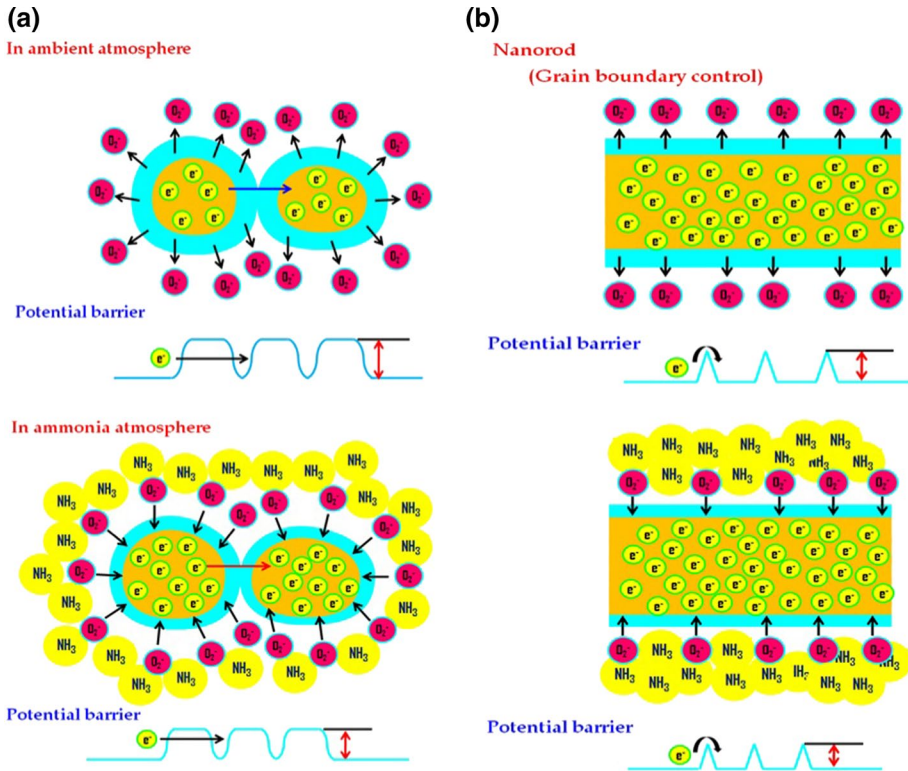


Fig. 8 NH_3 sensing mechanism towards **a** ZnO and **b** Al-ZnO (3wt.%) thin film

Hence, owing to its thin depletion layer, additional electrons are injected when NH_3 reacts with oxygen species.

4 Conclusions

In this present work, we report the sensor-based Al-doped ZnO films using the SILAR route. Aluminium ions were successfully incorporated into the ZnO structure which was confirmed from the XRD and further confirmation was carried out by EDX. The morphological analysis approves the development of nanowire like structure formed by dopant impurity which is favorable for sensing. The evaluated E_g varied from 3.01 to 3.12 eV on rising the Al doping content. RT ammonia sensing analysis showed an excellent response towards ammonia. In addition, the film doped with 3wt.% displays improvement in fast response and recovery characteristics. The outcomes signify that the grown Al-doped ZnO films are of great importance for gas sensing.

Acknowledgements The authors would like to express their gratitude to Deanship of Scientific Research at King Khalid University for funding this work through Research Groups Program under Grant No. R.G.P2/93/41.

References

- Abed, S., Bougharraf, H., Bouchouit, K., Sofiani, Z., Derkowska-Zielinska, B., Aida, M.S., Sahraoui, B.: Influence of Bi doping on the electrical and optical properties of ZnO thin films. *Superlattices Microstruct.* **85**, 370–378 (2015). <https://doi.org/10.1016/j.spmi.2015.06.008>
- Adel, H., Alkhayatt, O., Jaafer, M.D., Al Alak, H.H.A., Ali, A.H.: Characterization of CuO/n-Si pn junction synthesized by successive ionic layer adsorption and reaction method. *Opt. Quantum Electron.* **51**(7), 233 (2019). <https://doi.org/10.1007/s11082-019-1951-4>
- Ahmed, M.A.M., Meyer, W.E., Nel, J.M.: Effect of (Ce, Al) co-doped ZnO thin films on the Schottky diode properties fabricated using the sol-gel spin coating. *Mater. Sci. Semicond. Process.* **103**, 104612 (2019). <https://doi.org/10.1016/j.mssp.2019.104612>
- Anita, H., Kohli, N., Singh, R.C.: Temperature dependent selective and sensitive terbium doped ZnO nanostructures. *Sens. Actuators B* **231**, 110–119 (2016). <https://doi.org/10.1016/j.snb.2016.03.001>
- Antaryami Mohanta, J.G., Jr, Shen, S.G., Kim, S.M., Kung, P., Everitt, H.O.: Al doping in ZnO nanowires enhances ultraviolet emission and suppresses broad defect emission. *J. Lumin.* **211**, 264–270 (2019). <https://doi.org/10.1016/j.jlumin.2019.03.049>
- Aslani, A.: VahidOroojpour, CO gas sensing of CuO nanostructures, synthesized by an assisted solvothermal wet chemical route. *Phys. B* **406**, 144–149 (2011). <https://doi.org/10.1016/j.physb.2010.09.038>
- Aydın, H., Yakuphanoglu, F., Aydın, C.: Al-doped ZnO as a multifunctional nanomaterial: Structural, morphological, optical and low-temperature gas sensing properties. *J. Alloys Comp.* **773**, 802–811 (2019). <https://doi.org/10.1016/j.jallcom.2018.09.327>
- Benelmadjat, H., Boudine, B., Keffous, A., Gabouze, N.: Photo response and H₂ gas sensing properties of highly oriented Al and Al/Sb doped ZnO thin films. *Mater. Int.* **23**(6), 519–523 (2013). <https://doi.org/10.1016/j.pnsc.2013.11.001>
- Binjing, Hu., Sun, Q., Zuo, C., Pei, Y., Yang, S., Zheng, H., Liu, F.: A highly efficient porous rod-like Ce-doped ZnO photocatalyst for the degradation of dye contaminants in water. *Beilstein J. Nanotechnol.* **10**, 1157–1165 (2019). <https://doi.org/10.3762/bjnano.10.115>
- Chen, H.-I., Chi, C.-Y., Chen, W.-C., Liu, I.-P., Chang, C.-H., Chou, T.-C., Liu, W.-C.: *Sens. Actuators B: Chem.* **267**, 145–154 (2018). <https://doi.org/10.1016/j.snb.2018.04.019>
- Deshmukh, S.G., Kheraj, V., Panchal, A.K.: Preparation of nanocrystalline CdS thin film by successive ionic layer adsorption and reaction (SILAR) method. *Mater. Today: Proc.* **5** 21322–21327 (2018). <https://doi.org/10.1016/j.matpr.2018.06.535>
- Deva Arun Kumar, K., Ganesh, V., Valanarasu, S., Shkir, M., Kulandaisamy, I., Kathalingam, A., AlFaify, S.: Effect of solvent on the key properties of Al doped ZnO films prepared by nebulized spray pyrolysis technique. *Mater. Chem. Phys.* **212**, 167–174 (2018). <https://doi.org/10.1016/j.matchemphys.2018.03.035>
- Dilova, T., Atanasova, G., Dikovska, A. Og., Avdeev, G., Machida, M., Terakawa, M., Stefanov, P., Nedyalkov, N.N.: Effect of Pd-decoration on the sensing properties of ZnO nanostructures. *Thin Solid Films.* **693**, 137693 (2020). <https://doi.org/10.1016/j.tsf.2019.137693>
- Eisele, I., Doll, T., Burgmair, M.: Low power gas detection with FET sensors. *Sens. Actuators B* **78**, 19–25 (2001)
- Fairose, S., Ernest, S.: Nanostructured ZnO sensor fabricated by successive ionic layer adsorption and reaction method for ammonia sensing application. *Phys. B: Condensed Matter* **557** 63–73 (2019). <https://doi.org/10.1016/j.physb.2018.12.041>
- Fidal, V.T., Chandra, T.S.: Effect of neutral red incorporation on Al-doped ZnO thin films and its bio-electrochemical interaction with NAD⁺/NADP⁺ dependent enzymes. *Enzyme Microbial Technol.* **116**, 57–63 (2018). <https://doi.org/10.1016/j.enzmictec.2018.05.008>
- Firdous, A., Singh, D., Ahmad, M.M.: Electrical and optical studies of pure and Ni-doped CdS quantum dots. *Appl Nanosci.* **3** 13–18 (2013). <https://doi.org/10.1007/s13204-012-0065-0>
- Fu, Y., Luo, J., Du, X., Flewitt, A., Li, Y., Markx, G., Walton, A., Milne, W.: Recent developments on ZnO films for acoustic wave based bio-sensing and microfluidic applications: a review. *Sensors Actuators B Chem.* **143**, 606–619 (2010). <https://doi.org/10.1016/j.snb.2009.10.010>
- Ganesh Kumar Mani, John Bosco Balaguru, R.: Influence of copper doping on structural, optical and sensing properties of spray deposited zinc oxide thin films. *J. Alloy. Compd.* **582**, 414–419 (2014). <https://doi.org/10.1016/j.jallcom.2013.07.146>
- Ganesh Kumar Mani, John Bosco Balaguru Rayappan: A highly selective and wide range ammonia sensor—nanostructured ZnO: Co thin film. *Mater. Sci. Eng. B* **191**, 41–50 (2015). <https://doi.org/10.1016/j.mseb.2014.10.007>

- Ghosh, J., Ghosh, R., Giri, P.K.: Tuning the visible photoluminescence in Al doped ZnO thin film and its application in label-free glucose detection. *Sens. Actuators B* **254**, 681–689 (2018). <https://doi.org/10.1016/j.snb.2017.07.110>.
- Goktasa, A., Aslan, F., Tumbul, A., Gunduz, S.H.: Tuning of structural, optical and dielectric constants by various transition metal doping in ZnO:TM (TM=Mn Co, Fe) nanostructured thin films: A comparative study. *Ceramics Int.* **43**, 704–713 (2016). <https://doi.org/10.1016/j.ceramint.2016.09.217>
- Gopala Krishnan, V., Elango, P.: Influence of Ba doping concentration on the physical properties and gas sensing performance of ZnO nanocrystalline films: automated nebulizer spray pyrolysis (ANSP) method. *Optik Int. J. Light Electron Optics* **141**, 83–89 (2017). <https://doi.org/10.1016/j.ijleo.2017.05.045>.
- Hong, M.-H., Choi, H., Shim Ji, D., Cho, H.H., Park, H.-H.: Study of the effect of stress/strain of mesoporous Al-doped ZnO thin films on thermoelectric properties. *Solid State Sci.* **82**, 84–91 (2018). <https://doi.org/10.1016/j.solidstatesciences.2018.05.010>
- Hou, Y., Jayatissa, A.H.: Influence of laser doping on nanocrystalline ZnO thin films gas sensors. *Progr. Natural Sci. Mater. Int.* **27**, 435–442 (2017). <https://doi.org/10.1016/j.pnsc.2017.07.002>
- Humayan Kabir M., Al Amin, M., Rahman, M.S., Khan, M.K.R.: Influence of Al doping on microstructure, morphology, optical and photoluminescence properties of pyrolytic ZnO thin films prepared in an ambient atmosphere. *Chin. J. Phys.* **56**, 2275–2284 (2018). <https://doi.org/10.1016/j.cjph.2018.07.004>
- Kadhim, I.H., Abu Hassan, H.: Room temperature hydrogen gas sensor based on nanocrystalline SnO₂ thin film using sol–gel spin coating technique. *J Mater Sci: Mater Electron* **27**(5), 4356–4362 (2016). <https://doi.org/10.1007/s10854-016-4304-0>
- Kanaparthi, S., Singh, S.G.: Highly sensitive and ultra-fast responsive ammonia gas sensor based on 2D ZnO nanoflakes. *Mater. Sci. Energy Technol.* **3**, 91–96 (2020). <https://doi.org/10.1016/j.mset.2019.10.010>
- Kim, J.-H., Mirzaei, A., Kim, H.W., Kim, S.S.: Pd functionalization on ZnO nanowires for enhanced sensitivity and selectivity to hydrogen gas. *Sens. Actuators: B. Chem.* **297**, 126693 (2019). <https://doi.org/10.1016/j.snb.2019.126693>
- Kolhe, P.S., Shinde, A.B., Kulkarni, S.G., Maiti, N., Koinkar, P.M., Sonawane, K.M.: Gas sensing performance of Al doped ZnO thin film for H₂S detection. *J. Alloys Comp.* **748**, 6–11 (2018). <https://doi.org/10.1016/j.jallcom.2018.03.123>.
- Kulandaishamy, A.J., Reddy, J.R., Srinivasan, P., Jayanth, Babu K., Mani, G.K., Shankar, P., Rayappan, J.B.B.: Room temperature ammonia sensing properties of ZnO thin films grown by spray pyrolysis: Effect of Mg doping. *J. Alloys Compounds* **688**, 422–429 (2016). <https://doi.org/10.1016/j.jallcom.2016.07.050>
- Kwon, D.-K., Porte, Y., Myoung, J.-M.: Fabrication of ZnO nanorods p–n homojunction light-emitting diodes using Ag film as self-doping source for p-type ZnO nanorods. *J. Phys. Chem. C* **122**, 11993–12001 (2018). <https://doi.org/10.1021/acs.jpcc.8b02330>
- Linhua Xu, Shaorong Xiao, Chengyi Zhang, Gaige Zheng, Jing Su, Lilong Zhao, Junfeng Wang.: Optical and structural properties of Sr-doped ZnO thin films. *Mater. Chem. Phys.* **148** 720e726 (2014). <https://doi.org/10.1016/j.matchemphys.2014.08.040>.
- Linhua, Xu., Miao, J., Chen, Y., Jing, Su., Yang, M., Zhang, L., Zhao, L., Ding, S.: Characterization of Ag-doped ZnO thin film for its potential applications in optoelectronic devices. *Optik* **170**, 484–491 (2018). <https://doi.org/10.1016/j.ijleo.2018.06.016>
- Linhua, X., Wang, X., Xian, F., Jing, S.: Doping-induced transition from polycrystals to single crystals in ZnO thin films. *Mater. Res. Bull.* **123**, 110724 (2019). <https://doi.org/10.1016/j.materresbull.2019.110724>
- Liu, C.Y., Zhang, B.P., Lu, Z.W., Binh, N.T., Wakatsuki, K., Segawa, Y., Mu, R.: Fabrication and characterization of ZnO film based UV photodetector. *J Mater Sci: Mater Electron* **20**, 197–201 (2009). <https://doi.org/10.1007/s10854-008-9698-x>
- Liu, I.-P., Chang, C.-H., Chieh Chou, T., Lin, K.-W.: Ammonia sensing performance of a platinum nanoparticle-decorated tungsten trioxide gas sensor. *Sens Actuators: B. Chem.* **291**, 148–154 (2019). <https://doi.org/10.1016/j.snb.2019.04.046>
- Lupan, O., Vasile Postica, Thierry Pauporté, Bruno Viana, Maik-Ivo Terasa, Rainer Adelung.: Room temperature gas nanosensors based on individual and multiple networked Au-modified ZnO nanowires. *Sens. Actuators: B. Chem.* **299**, 126977 (2019). <https://doi.org/10.1016/j.snb.2019.126977>
- Madhumita Sinha, Rajat Mahapatra, Manas Kumar Mondal, Satheesh Krishnamurthy, Ranajit Ghosh.: Fast response and low temperature sensing of acetone and ethanol using Al-doped ZnO microrods. *Phys. E: Low-Dimensional Syst. Nanostruct.* **118**, 113868 (2020). <https://doi.org/10.1016/j.physe.2019.113868>.

- Mariappan, R., Ponnuswamy, V., Suresh, R., Suresh, P., Chandra Bose, A., Ragavendar, M.: Role of substrate temperature on the properties of Na-doped ZnO thin film nanorods and performance of ammonia gas sensors using nebulizer spray pyrolysis technique. *JALCOM* **582**, 387–391 (2014). <https://doi.org/10.1016/j.jallcom.2013.08.048>
- Mkawi, E.M., Ibrahim, K., Ali, M.K.M., Farrukh, M.A., Mohamed, A.S.: The effect of dopant concentration on properties of transparent conducting Al-doped ZnO thin films for efficient Cu₂ZnSnS₄ thin-film solar cells prepared by electrodeposition method. *Appl Nanosci.* **5**, 993–1001 (2015). <https://doi.org/10.1007/s13204-015-0400-3>
- Mhlongo, G.H., Motaung, D.E., Swart, H.C.: Pd²⁺ doped ZnO nanostructures: structural, luminescence and gas sensing properties. *Mater. Lett.* **160**, 200–205 (2015). <https://doi.org/10.1016/j.matlet.2015.07.139>
- Mohd Arif, Mohd Shkir, Salem AlFaify, Vanga Ganesh, Amit Sanger, Hamed Algarni, Paula M. Vilarinho, Arun Singh.: A structural, morphological, linear, and nonlinear optical spectroscopic studies of nanostructured Al-doped ZnO thin films: An effect of Al concentrations. *J. Mater. Res.* **34**, 1309–1317 (2019). <https://doi.org/10.1557/jmr.2018.506>
- Musaab Khudhr, M., Khalid Haneen A.: Effect of Al-doping on the optical properties of ZnO thin film prepared by thermal evaporation technique. *Int. J. Eng. Technol.* **7**, 25–31 (2016) <https://www.scipress.com/IJET.7.25>
- Nanto, H., Minami, T., Takata, S.: Zinc oxide thin film ammonia gas sensors with high sensitivity and excellent selectivity. *J. Appl. Phys.* **60**, 482 (1986). <https://doi.org/10.1063/1.337435>
- Nkosi, S.S., Kortidis, I., Motaung, D.E., Kroon, R.E., Leshabane, N., Tshilongo, J., Ndwandwe, O.M.: The effect of stabilized ZnO nanostructures green luminescence towards LPG sensing capabilities. *Mater. Chem. Phys.* **242**, 122452 (2020). <https://doi.org/10.1016/j.matchemphys.2019.122452>
- Nunes, D., Pimentel, A., Gonçalves, A., Pereira, S., Branquinho, R., Barquinha, P., Fortunato, E., Martins, R.: Metal oxide nanostructures for sensor applications. *Semiconductor Sci. Technol.* **34**, 043001 (2019). <https://doi.org/10.1088/1361-6641/ab011e>
- Osali, S., Esfahani, H., Karami, H.R.: Effect of Al doping on crystallography and electro-optical properties of ZnO semiconductor thin films prepared by electrospinning. *Solid State Sci.* **83**, 90–98 (2018). <https://doi.org/10.1016/j.solidstatesciences.2018.05.016>
- Patil, V.L., Vanalakar, S.A., Tarwal, N.L., Patil, A.P., Dongale, T.D., Kim, J.H., Patil, P.S.: Construction of Cu doped ZnO nanorods by chemical method for low temperature detection of NO₂ gas. *Sens. Actuators A* **299**, 111611 (2019). <https://doi.org/10.1016/j.sna.2019.111611>
- Qin, W., Li, T., Li, Y., Qiu, J., Ma, X., Chen, X., Xuefeng, Hu., Zhang, W.: A high power ZnO thin film piezoelectric generator. *Appl. Surf. Sci.* **364**, 670–675 (2016). <https://doi.org/10.1016/j.apsusc.2015.12.178>
- Rajendra Prasad, M., Haris, M., Sridharan, M.: NH₃ sensing properties of surface modified Ce-doped nanostructured ZnO thin films prepared by spray pyrolysis method. *Sens. Actuators A* **269** 435–443 (2018). <https://doi.org/10.1016/j.sna.2017.11.045>
- Rana, A.K., Rajasree, D., Kumar, Y., Sen, S., Shirag, P.M.: Growth of transparent Zn_{1-x}Sr_xO (0.0 ≤ x ≤ 0.08) films by facile wet chemical method: Effect of Sr doping on the structural, optical and sensing properties. *APSUSC* **379**, 23–32 (2016). <https://doi.org/10.1016/j.apsusc.2016.04.066>
- Raut, S.S., Bisen, O., Sankapal, B.R.: Synthesis of interconnected needle-like Bi₂O₃ using successive ionic layer adsorption and reaction towards super capacitor application. *Ionics* **23**(7), 1831–1837 (2017). <https://doi.org/10.1007/s11581-017-1994-0>
- Ravichandran, K., Manivasaham, A., Subha, K., Chandrabose, A., Mariappan, R.: Cost-effective nebulizer sprayed ZnO thin films for enhanced ammonia gas sensing—effect of deposition temperature. *Surfaces Interfaces* **1–3**, 13–20 (2016). <https://doi.org/10.1016/j.surfin.2016.06.004>
- Ravichandran, R., JansiSanthosam, A., Sridharan, M.: Effect of tungsten doping on the ammonia vapour sensing ability of ZnO thin films prepared by a cost effective simplified spray technique. *Surfaces Interfaces* **18**, 100412 (2019). <https://doi.org/10.1016/j.surfin.2019.100412>
- Renitta, A., Vijayalakshmi, K.: High performance hydrogen sensor based on Mn implanted ZnO nanowires array fabricated on ITO substrate. *Mater. Sci. Eng. C* **77**, 245–256 (2017). <https://doi.org/10.1016/j.msec.2017.03.234>
- Rudra, K., Prajapati, Y.K.: Effect of Mn doping on defect-related photoluminescence and nanostructure of dense 3-D nano-root network of ZnO. *Ceramics Int.* **46**, 10135–10141 (2020). <https://doi.org/10.1016/j.ceramint.2020.01.004>
- Sankar Ganesh, R., Durgadevi, E., Navaneethan, M., Patil, V.L., Ponnusamy, S., Muthamizhchelvan, C., Kawasaki, S., Patil, P.S., Hayakawa, Y.: Low temperature ammonia gas sensor based on Mn-doped ZnO nanoparticle decorated microspheres. *J. Alloy. Comp.* **721** 182–190 (2017a). <https://doi.org/10.1016/j.jallcom.2017.05.315>

- Sankar Ganesh, R., Navaneethan, M., Mani, Ganesh Kumar, Ponnusamy, S., Tsuchiya, K., Muthamizhchelvan, C., Kawasaki, S., Hayakawa, Y.: Influence of Al doping on the structural, morphological, optical, and gas sensing properties of ZnO nanorods. *J. Alloys Compounds* **698**, 555–564 (2017b). <https://doi.org/10.1016/j.jallcom.2016.12.187>
- Sankar Ganesh, R., Durgadevi, E., Navaneethan, M., Patil, V.L., Ponnusamy, S., Muthamizhchelvan, C., Kawasaki, S., Patil, P.S., Hayakawa, Y.: *Chem. Phys. Lett.* **689**, 92–99 (2017c). <https://doi.org/10.1016/j.cplett.2017.09.057>
- Sankar Ganesh, R., Navaneethan, M., Patil, V.L., Ponnusamy, S., Muthamizhchelvan, C., Kawasaki, S., Patil, P.S., Hayakawa, Y.: Sensitivity enhancement of ammonia gas sensor based on Ag/ZnO flower and nanoellipsoids at low temperature. *Sens. Actuators B: Chem.* **255**, 672–683 (2017d). <https://doi.org/10.1016/j.snb.2017.08.015>
- Sankar Ganesh, R., Durgadevi, E., Navaneethan, M., Patil, V.L., Ponnusamy, S., Muthamizhchelvan, C., Kawasaki, S., Patil, P.S., Hayakawa, Y.: Tuning the selectivity of NH₃ gas sensing response using Cu-doped ZnO nanostructures. *Sens. Actuators A* **269**, 331–341 (2017e). <https://doi.org/10.1016/j.sna.2017.11.042>
- Sberveglieri, G., Groppelli, S., Nelli, P., Tintinelli, A., Giunta, G.: A novel method for the preparation of NH₃ sensors based on ZnO-In thin films. *Chem. Sens. Actuators B* **24–25** 588–590 (1995).
- Schmidt-Mende, L., MacManus-Driscoll, J.L.: ZnO—nanostructures, defects, and devices. *Mater. Today*, **10**, 40–48 (2007).
- Shaaban, E. R., Abbady, G.H., El Sayed Yousef, Ali, G.A.M., Mahmoud, S.A., Afify, N.: Structural, optical and magnetic properties of Gd-doped ZnO thin films for spintronics applications. *Optoelectronics Adv. Mater. Rapid Commun.* **13**, 235–242 (2019)
- Sheeba, N.H., Vattappalam, S.C., Okram, G.S., Sharma, V., Sreenivasan, P.V., Mathew, S., Reena Philip, R.: *Mater. Res. Bull.* **93**, 130–137 (2017). <https://doi.org/10.1016/j.materresbull.2017.04.021>
- Sinha, M., Mahapatra, R., Mondal, M.K., Krishnamurthy, S., Ghosh, R.: Fast response and low temperature sensing of acetone and ethanol using Al-doped ZnO microrods. *Physica E* (2020). <https://doi.org/10.1016/j.physe.2019.113868>
- Sivalingam, D., Jeyaprakash, B.G., John Bosco Balaguru, R.: Structural, morphological, electrical and vapour sensing properties of Mn doped nanostructured ZnO thin films. *Sens. Actuators B: Chem.* **166–167** 624–631 (2012)
- Stegmeier, S., Fleischer, M., Tawil, A., Hauptmann, P., Egly, K., Rose, K.: Sensing mechanism of room temperature CO₂ sensors based on primary amino groups. *Sens. Actuators B* **154**, 270–276 (2011). <https://doi.org/10.1016/j.snb.2010.01.022>
- Taabouche, A., Bouabellou, A., Kermiche, F., Hanini, F., Sedrati, C., Bouachiba, Y., Benazzouz, C.: Preparation and characterization of Al-doped ZnO piezoelectric thin films grown by pulsed laser deposition, *Ceramics International* (2016). <https://doi.org/10.1016/j.ceramint.2016.01.033>.
- Vijayprasath, G., Murugan, R., Ravi, G., Mahalingam, T., Hayakawa, Y.: Characterization of dilute magnetic semiconducting transition metal doped ZnO thin films by sol-gel spin coating method. *Appl. Surf. Sci.* **313**, 870–876 (2014)
- Vinoth, E., Gopalakrishnan, N.: Ammonia sensing characteristics of Yttrium doped ZnO thin films by RF magnetron sputtering. *Mater. Res. Express* (in press). <https://doi.org/10.1088/2053-1591/aac99a>.
- Viter, R., Iatsunskyi, I.: Metal oxide nanostructures in sensing, nanomaterials design for sensing applications. *Micro Nano Technol.*, pp 41–91. <https://doi.org/10.1016/B978-0-12-814505-0.00002-3>.
- Wagh, M.S., Jain, G.H., Patil, D.R., Patil, S.A., Patil, L.A.: Modified zinc oxide thick film resistors as NH₃ gas sensor. *Sens. Actuators B* **115**, 128–133 (2006). <https://doi.org/10.1016/j.snb.2005.08.030>
- Wang, Y., Chen, Y., Song, X., Zhang, Z., She, J., Deng, S., Ningsheng, Xu., Chen, J.: Electrical properties of fluorine-doped ZnO nanowires formed by biased plasma treatment. *Phys. E* (2018). <https://doi.org/10.1016/j.physe.2018.01.028>
- Yuanyuan Lv, Zhiyong Zhang, Junfeng Yan, Wu Zhao, Chunxue Zhai.: Al doping influences on fabricating ZnO nanowire arrays enhanced field emission property. *Ceramics Int.* <https://doi.org/10.1016/j.ceramint.2018.01.118>.
- Zaiour, A., Benhaya, A., Bentrucia, T.: Impact of deposition methods and doping on structural, optical and electrical properties of ZnO-Al thin films. *Optik Int. J. Light Electron Optics* **186**, 293–299 (2019). <https://doi.org/10.1016/j.ijleo.2019.04.132>
- Zhai, C.-H., Zhang, R.-J., Chen, X., Zheng, Y.-X., Wang, S.-Y., Liu, J., Dai, N., Chen, L.-Y.: Effects of Al doping on the properties of ZnO thin films deposited by atomic layer deposition. *Nanoscale Res. Lett.* (2016). <https://doi.org/10.1186/s11671-016-1625-0>

- Zhang, B., Gao, P.-X.: Metal oxide nanoarrays for chemical sensing: a review of fabrication methods, sensing modes, and their inter-correlations. *Front. Mater.* (2019). <https://doi.org/10.3389/fmats.2019.00055>
- Zhang, Y.-H., Li, Y.-L., Gong, F.-L., Xie, K.-F., Liu, M., Zhang, H.-L., Fang, S.-M.: Al doped narcissus-like ZnO for enhanced NO₂ sensing performance: an experimental and DFT investigation. *Sens. Actuators: B. Chem.* (2019). <https://doi.org/10.1016/j.snb.2019.127489>
- Zhijie Li, Hao Li, Zhonglin Wu, Mingkui Wang, Jingting Luo, Hamdi Torun, PingAn Hu, Chang Yang, Marius Grundmann, Xiaoteng Liu, YongQing Fu.: Advances in designs and mechanisms of semi-conducting metal oxide nanostructures for high-precision gas sensors operated at room temperature. *Mater. Horiz.*, **6**, 470–506 (2019). <https://doi.org/10.1039/c8mh01365a>.
- Zouhair Sofiani, Bouchta Sahraoui, Mohammed Addou, Rahma Adhiri, Mehdi Alaoui Lamrani, Leila Dghoughi, Nabil Fellahi, Beata Derkowska, Waclaw Bala.: Third harmonic generation in undoped and X doped ZnO films (X: Ce, F, Er, Al, Sn) deposited by spray pyrolysis. *J. Appl. Phys.* **101**(6), 063104–063104-5 (2007). <https://doi.org/10.1063/1.2711143>

Publisher's Note Springer Nature remains neutral with regard to jurisdictional claims in published maps and institutional affiliations.